Journal of Pharmaceutical and Biomedical Analysis 266 (2025) 117091

Contents lists available at ScienceDirect

Journal of Pharmaceutical and Biomedical Analysis

journal homepage: www.journals.elsevier.com/journal-of-pharmaceutical-and-biomedical-analysis

Non-targeted metabolite characterization in microsomal assay using liquid chromatography coupled to high-resolution mass spectrometry: Application to carisoprodol

Elena Ferri [a,b], Cristian Caprari [a,c], Maria Angela Vandelli [a], Loretta L. Del Mercato [d], Cinzia Citti [a,d,*], Giuseppe Cannazza [a,d]

[a] Department of Life Sciences, University of Modena and Reggio Emilia, Via Campi 103, Modena 41125, Italy
[b] Health Innovative Products and Technologies (HIP-TECH) PhD Program, Department of Life Sciences, University of Modena and Reggio Emilia, Modena 41125, Italy
[c] Clinical and Experimental Medicine (CEM) PhD Program, Nanomedicine, Medicinal and Pharmaceutical Sciences, Department of Life Sciences, University of Modena and Reggio Emilia, Modena 41125, Italy
[d] Institute of Nanotechnology – CNR NANOTEC, Campus Ecotekne, Via Monteroni, Lecce 73100, Italy

ARTICLE INFO

Keywords:
Carisoprodol
Metabolite prediction
Hydroxy carisoprodol
Meprobamate
High-resolution mass spectrometry

ABSTRACT

Understanding the metabolic fate of pharmaceutical compounds is critical for assessing drug safety and efficacy. A combination of advanced analytical techniques and *in vitro* models allows for detailed investigation of biotransformation processes. This study presents an integrated workflow using carisoprodol as a case study to demonstrate the application of modern analytical strategies for metabolic profiling. An analytical platform based on liquid chromatography–high-resolution mass spectrometry (LC-HRMS) was employed, operating in both MS^1 and MS^2 modes to investigate fragmentation behaviour and identify metabolites. Chromatographic separation was performed using a core-shell C_{18} column under gradient elution. *In vitro* metabolic stability studies were conducted using rat liver microsomes, and a deuterated analogue was also tested to assist in structural elucidation of hydroxylated metabolites. Additionally, *in silico* metabolite prediction tools were applied and compared with experimental results. The compound showed slow metabolic degradation ($t_{1/2}$ = 233.72 ± 3.09 min) and low intrinsic clearance ($CL_{int,\ in\ vitro}$ = 5.930 ± 0.078 μL/min/mg). LC-HRMS enabled identification of meprobamate and a hydroxylated derivative as major metabolites. MS/MS analysis of the deuterated metabolite excluded hydroxylation on the *n*-pentyl chain as reported in the literature, indicating alternative modification sites. *In silico* predictions correctly identified meprobamate but misassigned hydroxylation positions for the other metabolite. This study highlights the effectiveness of a multi-technique analytical approach for elucidating drug metabolism. The integration of LC-HRMS, isotopic labelling, and computational tools provides a comprehensive platform for metabolic characterization, while emphasizing the necessity of experimental validation in refining *in silico* predictions.

1. Introduction

Pharmacokinetic studies play a pivotal role in understanding the absorption, distribution, metabolism, and excretion (ADME) of therapeutic agents. They are essential for predicting drug efficacy, safety profiles, potential interactions, and risks of accumulation or toxicity. In particular, investigating the metabolic pathways of centrally acting drugs is critical to accurately interpret their pharmacological and toxicological profiles.

Carisoprodol, chemically known as (2*RS*)-2-[(Carbamoyloxy) methyl]-2-methylpentyl(1-methylethyl)carbamate (or *N*-isopropyl meprobamate) (Fig. 1A), was developed by Dr. Frank M. Berger as a muscle relaxant in 1959. It was specifically synthesized to enhance muscle relaxation while offering improved safety and a lower potential for abuse compared to meprobamate (1,3-propanediol, 2-methyl-2-propyl-, 1,3-dicarbamate) (Fig. 1B) [1].

Carisoprodol is a widely prescribed medicine in several countries. In the United States, it is a controlled prescription drug, classified as a

* Corresponding author at: Institute of Nanotechnology – CNR NANOTEC, Campus Ecotekne, Via Monteroni, Lecce 73100, Italy.
E-mail addresses: elena.ferri@unimore.it (E. Ferri), cristian.caprari@unimore.it (C. Caprari), mariaangela.vandelli@unimore.it (M.A. Vandelli), loretta.delmercato@cnr.it (L.L. Del Mercato), cinzia.citti@cnr.it (C. Citti), giuseppe.cannazza@unimore.it (G. Cannazza).

https://doi.org/10.1016/j.jpba.2025.117091
Received 15 May 2025; Received in revised form 31 July 2025; Accepted 4 August 2025
Available online 7 August 2025

Schedule IV substance under the Controlled Substances Act since January 2012. In contrast, its use has been progressively restricted in Europe due to safety concerns [2]. Sweden withdrew the drug in 2007, followed by Norway in 2008, where its ban led to a decrease in impaired driving cases, intoxications, and related fatalities. Subsequently, the European Medicines Agency (EMA) recommended the suspension of the marketing authorisations of medicinal products containing carisoprodol [3,4].

At the international level, the 47th Expert Committee on Drug Dependence (ECDD) in 2024 recommended adding carisoprodol to Schedule IV of the 1971 Convention on Psychotropic Substances [4].

Carisoprodol is administered orally in tablet form, with a standard adult dosage of 250–350 mg taken three times daily and at bedtime. Due to its potential for abuse and dependence, treatment duration should not exceed two to three weeks [5,6].

Carisoprodol is rapidly absorbed after oral administration, with effects beginning within 30–60 min and peak plasma concentration reached in 1.5–1.7 h. Its action lasts approximately 4–6 h, and bioavailability studies report a high absorption rate (92 %) [7]. Following a single 350 mg dose, peak plasma levels reach around 2580 ng/mL, with an elimination half-life of about 2 h. No significant accumulation occurs with prolonged use (350 mg every 8 h for 14 days), differently from its primary metabolite, meprobamate, which tends to accumulate [8].

Carisoprodol is moderately distributed in body tissues, crosses the placenta, and is excreted in breast milk. Its volume of distribution ranges between 0.93 and 1.3 L/kg, slightly higher for meprobamate (1.4–1.6 L/kg) [9].

Carisoprodol is extensively metabolized in the liver, primarily by the CYP2C19 enzyme, which converts it into its main metabolite, meprobamate. A multiethnic study by Hicks et al. [10] highlighted significant variability in CYP2C19 metabolic rates among individuals, with 2.1–27.1 % classified as rapid metabolizers, 19–45.9 % as intermediate metabolizers, and 1.4–57.1 % as poor metabolizers.

In individuals with reduced CYP2C19 activity, carisoprodol exposure can increase up to fourfold, while its conversion to meprobamate decreases by 50 % [11]. Clinical studies have also shown that intermediate metabolizers exhibit a 45 % higher carisoprodol concentration compared to rapid metabolizers.

Several external factors can further influence the drug's plasma levels: oral contraceptives can increase them by 60 %, while CYP2C19 inhibitors (such as omeprazole, fluoxetine, and sertraline) prolong its effects. Conversely, enzyme inducers (such as rifampin, phenobarbital, and St. John's wort) reduce its plasma concentration [12].

While the elimination half-life of carisoprodol is short, meprobamate has a much longer half-life (about 10 h), contributing to its persistence in the body [4]. Renal excretion is the primary elimination route, and impaired kidney function may slow this process. Most individuals rapidly metabolize carisoprodol, converting it almost entirely into meprobamate within 2.5 h, though slow metabolizers may take over 6 h, with reduced meprobamate conversion [13].

Meprobamate, derived from carisoprodol, enhances neuronal inhibition by acting on GABA-A receptors, similar to benzodiazepines and barbiturates, producing sedative and hypnotic effects. However, evidence suggests that carisoprodol also exerts direct effects on the central nervous system, independent of meprobamate, though its precise mechanism remains unclear [1]. From a behavioural perspective, carisoprodol induces motor-depressant effects similar to barbiturates, independent of meprobamate, as its duration of action is much shorter than the metabolite's plasma half-life [14]. Pharmacological discrimination studies confirm a distinct mechanism of action, as carisoprodol's effects are blocked by barbiturate antagonists but not by benzodiazepine antagonists [14].

Beyond meprobamate, hydroxy carisoprodol has been identified as a major metabolite, though its pharmacological role remains unclear [15].

Carisoprodol and its most studied metabolite, meprobamate, are aliphatic compounds with minimal UV absorbance or fluorescent properties, making their quantification primarily reliant on gas chromatography (GC) and gas chromatography coupled with mass spectrometry (GC-MS). However, both compounds are thermolabile, necessitating derivatization to enhance thermal stability and more accurate and reproducible analysis [1]. To overcome these limitations, liquid chromatography coupled with tandem mass spectrometry (LC-MS/MS) or high-resolution mass spectrometry (HRMS) is preferred, particularly for analysing biological fluids such as blood, urine, bile, muscle, liver, and plasma [4,16].

Carisoprodol is rapidly metabolized, and its plasma and urine concentrations are in ng/mL range, which can make its detection in biological samples challenging. As a result, meprobamate, classified as a controlled substance in some countries, is often the only detectable metabolite. It is therefore likely that cases of carisoprodol consumption are underestimated, as they may be attributed to meprobamate use [4].

Few studies have investigated the identification of carisoprodol metabolites in humans, with most research focusing on measuring simultaneous concentrations of carisoprodol and meprobamate following carisoprodol administration. Interestingly, metabolic studies in animal urine suggest that meprobamate is not the primary metabolite [15]. The first pharmacokinetic studies conducted in the early 1960s suggested that hydroxy carisoprodol was the main metabolite of carisoprodol found in urine and plasma [15]. Initial attempts to identify the structure of this metabolite indicated that a hydroxyl group replaced the C4 position in the *n*-pentyl chain as shown in Fig. 1C. Later, only a few studies confirmed the formation of hydroxy carisoprodol following carisoprodol administration and even fewer studies dealt with the quantitative determination of this metabolite [17,18].

In this study, we developed an LC-HRMS method to analyze carisoprodol and its metabolites following incubation with rat liver microsomes. The *in vitro* pharmacokinetic profile was evaluated, and major metabolites were tentatively identified, aiming to better understand the biotransformation of carisoprodol and contribute to the broader assessment of its pharmacological and toxicological behavior.

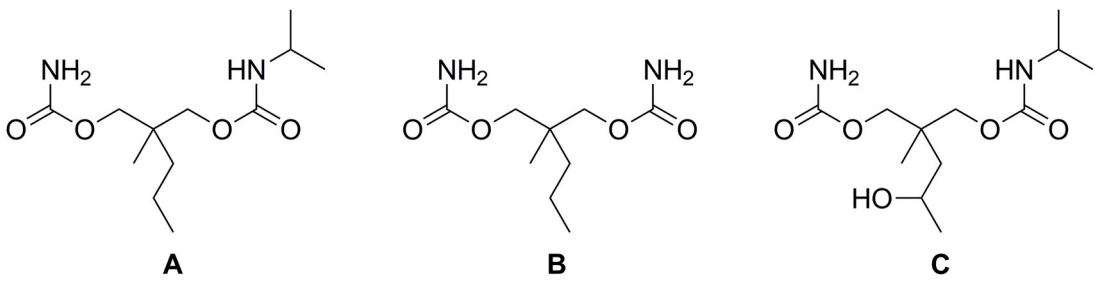

Fig. 1. Chemical structures of the investigated analytes. Chemical structure of carisoprodol (A), meprobamate (B), hydroxy carisoprodol (C) (according to the structure proposed in the literature).

2. Materials and methods

2.1. Chemicals and materials

LC-MS grade acetonitrile (ACN) and formic acid (FA) were purchased from Honeywell (Charlotte, North Caroline, USA). Ultrapure water for HPLC-HRMS analyses was obtained with a water purification system (Direct-Q 3UV, Merck Millipore, Milan, Italy). The pure standard of carisoprodol and testosterone (experimental control) were provided from Sigma Aldrich Merck (Milan, Italy).

A volume of 0.5 mL of rat liver microsomes (Sprague Dawley), pooled from twenty-five donors and with a protein concentration of 20 mg/mL, was obtained from Thermo Fisher Scientific (Gibco) and stored at −70°C. KH_2PO_4 and K_2HPO_4 were obtained from Sigma Aldrich Merck (Milan, Italy). Each salt was prepared as a 0.2 M solution and used to produce a 0.1 M potassium phosphate buffer by adding an appropriate amount of Milli-Q water. The buffer was stored at room temperature until incubation. Nicotinamide adenine dinucleotide phosphate (NADPH), used as a cofactor, was obtained from BLD Pharmatech GmbH (Reinbek, Germany) and, finally, deuterated carisoprodol-d_7, used as an internal standard (IS), was sourced from Sigma-Aldrich Merck (Milan, Italy).

2.2. In silico metabolite prediction

The metabolites of carisoprodol were predicted using GLORYx, a web-based machine learning model for simulating phase I and phase II metabolic reactions in humans. GLORYx is hosted on the New E-Resource for Drug Discovery (NERDD), a rapidly expanding portal that provides peer-reviewed *in silico* tools for drug discovery [19]. For the analysis, a simplified molecular input line entry system (SMILES), generated using ACD/ChemSketch [20], was used in the "phase I metabolism" option in GLORYx [21]. The metabolites with the major highest probability score were then incorporated in an inclusion list for LC-HRMS/MS analysis.

2.3. Incubation with pooled Rat Liver Microsomes (RLM)

Carisoprodol was incubated with cryopreserved rat microsomes using a previously described protocol with marginal changes where necessary [22]. To summarize, 26 µL of microsome suspension were gently mixed with 10 µL of carisoprodol (1 mg/mL stock solution) in phosphate buffer (864 µL) and cofactor NADPH 10 mM (100 µL) using MTH-100 Thermo Shaker incubator (MIULAB, Hangzhou, Zhejiang, Cina). Testosterone (used as a positive control) and negative controls were incubated alongside. A 100 µL aliquot of incubates was quenched with 50 µL of ice-cold acetonitrile containing internal standard (IS) carisoprodol-d_7, centrifuged for 10 min at 13,000 × *g* with MiniSpin centrifuge (Eppendorf SE, Hamburg, Germany) and then analysed. All reactions were conducted under physiological conditions (37 °C, pH 7.4). Following centrifugation, the supernatant was transferred into HPLC tubes and a 5 µL aliquot was injected into the LC-HRMS system.

The incubation reactions were carried out for a total of 180 min and monitored at fixed time points (0, 30, 60, 120, and 180 min). Testosterone was used as the positive control, while negative control samples were obtained without the addition of NADPH.

The same experiment was repeated using carisoprodol-d_7 as test compound to attempt identification of the correct position of the hydroxyl group in hydroxy carisoprodol.

2.4. LC/HRMS analysis of carisoprodol and its metabolites

Metabolite analyses were performed using an LC-HRMS system from Thermo Fisher Scientific (Waltham, MA, USA), equipped with an Ultimate 3000 ultra-high performance liquid chromatograph (UHPLC) and a Q-Exactive quadrupole-Orbitrap high-resolution mass spectrometer with a heated electrospray ionization (HESI) source. The UHPLC system included a binary pump, a vacuum degasser, a thermostated autosampler set at 7 °C, and a thermostated column compartment set at 25 °C. The mass spectrometer operated in positive ionization mode for data acquisition.

The chromatographic separations were achieved on a Poroshell 120 EC-C18 (100 × 3.0 mm I.D., 2.7 µm) with a guard (5 × 3 mm I.D., 2.7 µm) (both from Agilent Technologies, Milan, Italy). A gradient elution of water and ACN (both with 0.1 % formic acid) was set: a linear increase from 5 % to 95 % ACN was programmed from 2.0 to 20.0 min, held at 95 % for 5 min, and taken back to 5 % at 25.1 min. The column was re-equilibrated with 5 % ACN for 5 min and the run was stopped at 30 min.

The Orbitrap mass analyzer was set in full scan (FS) mode over an *m/z* range of 50–750. Data-dependent acquisition (DDA) was performed on quality control samples and used exclusively for MS/MS acquisition to obtain fragmentation spectra of the parent compound and its major metabolites.

For the HESI source the parameters were set as follows: capillary temperature, 320 °C; vaporizer temperature, 300 °C; voltage, 3.8 kV; sheath gas, 55 arbitrary units (au); auxiliary gas, 30 au; S lens RF level, 55 au. The orbitrap was fully calibrated before the analysis, with a lock mass list used for better accuracy. Data acquisition was carried out using Xcalibur 3.0 software (Thermo Fisher Scientific, San Jose, CA, USA) in full-scan and data-dependent MS/MS modes, covering a time range of 1–30 min. In full-scan MS mode, the automatic gain control (AGC) target was set to 3×10^6, with a resolution of 140,000 at full width at half maximum (FWHM) at 15 s. The maximum injection time (IT) was 500 ms, and the scan range in positive ionization mode covered *m/z* 50–750. For data-dependent MS/MS analysis, the AGC target was set to 5×10^5, with a minimum threshold of 1×10^3, a resolution of 17,500, a maximum IT of 100 ms, and an isolation window of *m/z* 0.4. The normalized collision energy (NCE) was set to 20 AU, with a loop count of 2 and a dynamic exclusion duration of 5.0 s. All analyses were processed using FreeStyle 1.8 (Thermo Fisher Scientific).

2.5. Identification of carisoprodol metabolites

The identification of carisoprodol and its metabolites was carried out by Compound Discoverer 3.3 (Thermo Fisher Scientific, Waltham, MA, USA). The workflow "MetID" suggested by the software was employed for the identification of metabolites of carisoprodol [23].

The processing workflow 1. performs retention time (R_T) alignment across all the samples; 2 detects expected compounds from *in silico* predictions for carisoprodol parent compounds based on its dealkylation and phase-1 metabolism products. Uses resolution-aware isotope pattern matching to confirm the formulas of the expected compounds it finds; 3. groups expected compounds across all the samples; 4. applies FISh (fragment ion search) scoring to all expected compounds and their transformation products; 5. annotates the fragmentation mass spectra for these compounds with structures and a FISh score; 6. predicts the elemental compositions for all unknown compounds, fills gaps across all samples, and hides the chemical background (by using Blank samples); 7. uses the Compound Class Scoring node to flag unknown compounds that share common fragments; 8. calculates mass defects for each compound. The workflow used is reported in Figure S1 (Supplementary Material).

2.6. Estimating the intrinsic clearance (CL_{int}) of carisoprodol

To estimate the CL_{int} of carisoprodol, the average of triplicate peak area ratios obtained from the metabolic stability assay at each non-zero-time intervals was normalized to the corresponding value obtained at the 0 min time point to yield the percentage of carisoprodol remaining at each time point. Thereafter, these resulting data points were plotted against its respective incubation time and the data was fitted to a one

phase exponential decay model using GraphPad Prism 8.0.1 (San Diego, CA) to determine its elimination rate constant (k). This allowed the *in vitro* half-life ($t_{1/2}$) of carisoprodol to be calculated using $t_{1/2}\ (min) = ln\ (2)/k$ [24].

Subsequently, the $CL_{int,\ in\ vitro}$ of carisoprodol can be further computed using the following equation:

$$CL_{int,\ in\ vitro}\ (\mu l/min/mg) = V \times 0.693/\ t_{1/2}$$

where V (µl/mg) corresponds to the volume of the incubation (in µl) divided by the protein amount in the incubation (mg) [22].

Based on the determined $CL_{int,\ in\ vitro}$, the corresponding *in vivo* intrinsic clearance ($CL_{int,\ in\ vivo}$) was also estimated using the following approach:

$$CL_{int,\ in\ vivo}\ (\mu l/min/mg) = CL_{int,\ in\ vitro} \times m_{microsomes}/g_{liver} \times m_{liver}/\ kg_{per\ body\ weight}$$

where $m_{microsomes}$ is 61 mg and represents the mass of the microsome per grams of liver (g_{liver}) for rat. The m_{liver} is assumed to be 40 g/kg, representing the amount of liver mass contained in each kg of body weight ($kg_{per\ body\ weight}$) in rats [25].

3. Results and discussion

3.1. LC-HRMS/MS analysis of carisoprodol

Using a gradient-based chromatographic method with acetonitrile and water (0.1 % formic acid) as mobile phases and a C18 core-shell column, carisoprodol eluted at 11.62 min. In positive ESI mode, the molecular ion $[M+H]^+$ was observed at m/z 261.1809, along with the sodium adduct at m/z 283.1628. Four fragment ions (a–d) generated by in-source fragmentation were attributed to specific bond cleavages (Fig. 2A and B). Two of these fragments, *a* and *c*, at m/z 200.1642 and 158.1174 respectively, were attributed to the cleavage of either the C2–O or C8-O bonds, respectively. Additionally, an ion *b* at m/z 176.1279, corresponding to the cleavage of the carbonyl C3–O bond, and an ion *d* at m/z 97.1015, corresponding to the simultaneous cleavage of both C2–O and C8-O bonds, were detected. The same in-source fragmentation profile was observed for carisoprodol-d_7 with additional 7.0439 amu on each fragment as reported in Fig. 2C. Carisoprodol-d_7 showed a similar fragmentation profile with a consistent mass shift of + 7.0439 amu (Fig. 2C). The MS/MS fragmentation spectra of the carisoprodol and carisoprodol-d_7 molecular ions are shown in Fig. 2D and E respectively. The structure corresponding to the fragments was tentatively identified and is reported in the fragmentation spectra in the figure. The *a*, *b*, *c*, and *d* fragments already described for in-source fragmentation are also visible in the MS/MS spectra. Detailed structure of each fragment generated in the MS^2 spectrum of carisoprodol is reported in Figure S2 (Supplementary Material).

3.2. In vitro metabolic stability studies

To evaluate the metabolic stability of carisoprodol in pooled rat liver microsomes (RLM), a previously developed protocol was applied with minor modifications [22], determining its *in vitro* half-life ($t_{1/2}$), intrinsic clearance *in vitro* ($CL_{int,\ in\ vitro}$), and estimated intrinsic clearance *in vivo* ($CL_{int,\ in\ vivo}$).

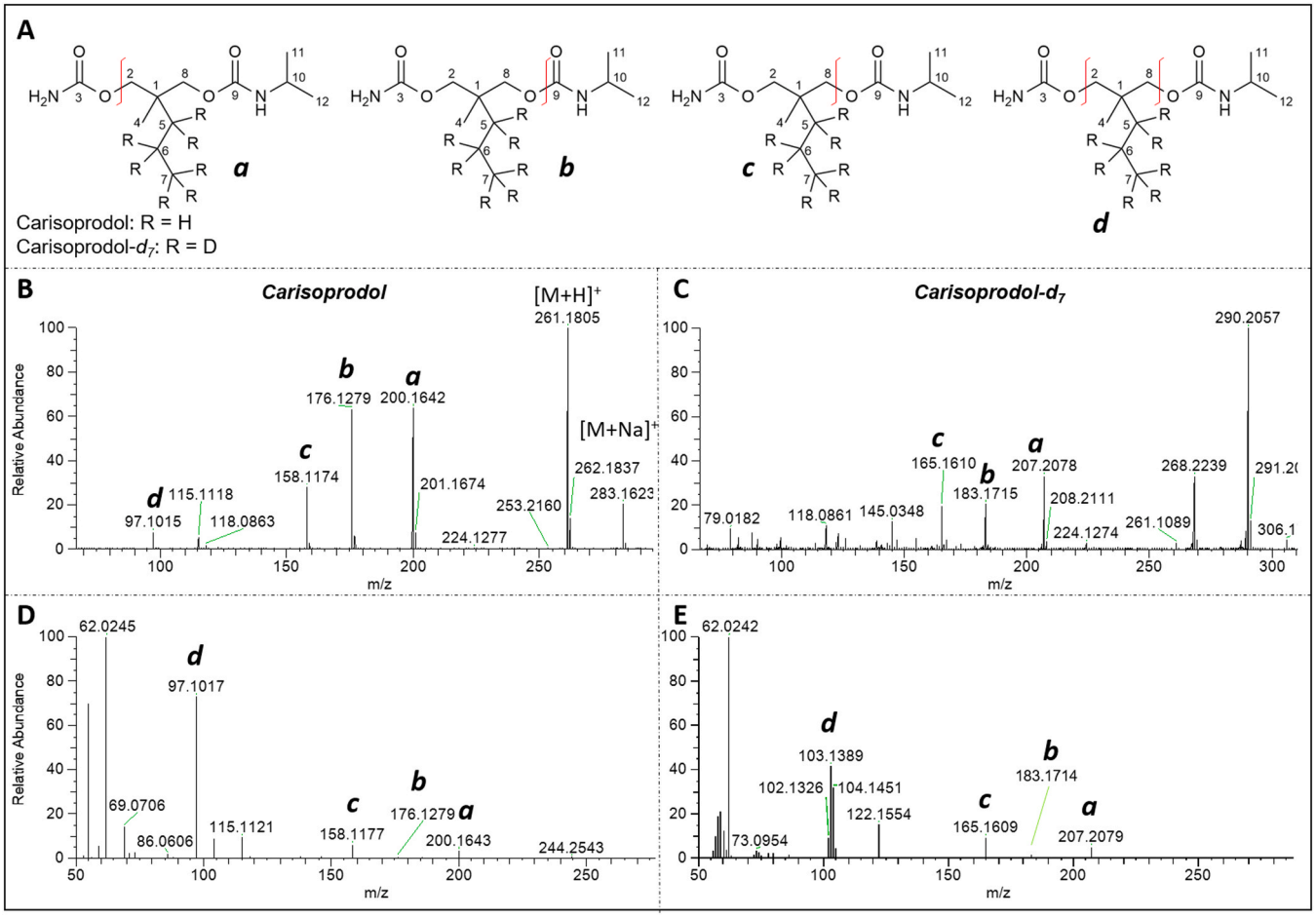

Fig. 2. In-source and MS^2 fragmentation pattern of carisoprodol and carisoprodol-d_7. Proposed fragmentation pattern for carisoprodol and carisoprodol-d_7 (A); in-source (MS^1) fragmentation spectrum of carisoprodol (B) and carisoprodol-d_7 (C); MS^2 fragmentation pattern of carisoprodol (D) and carisoprodol-d_7 (E).

Preliminary tests conducted on carisoprodol at various concentrations and time points suggested that carisoprodol concentration remained stable after 15 min, indicating that incubation times of at least 30 min were required to observe any significant metabolic degradation of the molecule. Therefore, the parent compound was incubated for 30, 60, 120, and 180 min. The logarithmic percentage decrease of carisoprodol is shown in the graph, representing the average of the data from three biological replicates (Fig. 3A).

Its concentration declined following pseudo-first-order kinetics (Fig. 3A) with a correlation factor (R^2) of 0.98 (Fig. 3B). The *in vitro* elimination half-life ($t_{1/2}$), *in vitro* intrinsic clearance ($CL_{int,\ in\ vitro}$), and the estimated *in vivo* intrinsic clearance ($CL_{int,\ in\ vivo}$) were calculated for the microsomal model as reported in the experimental section (Paragraph 2.6). The elimination rate constant (k) resulted 0.0030 ± 0.00013 min^{-1} , corresponding to an *in vitro* half-life ($t_{1/2}$) of 233.72 ± 3.09 min (CV%=0.013). Consequently, its $CL_{int\ in\ vitro}$ was determined to be 5.930 ± 0.078 µL/min/mg (CV%=0.013), and its $CL_{int\ in\ vivo}$ was estimated to be 14.47 ± 0.19 mL/min/kg (CV%=0.013), which is very close to the only available *in vivo* clearance data for carisoprodol, equal to 0.79 ± 0.29 L/h/kg (i.e., 13.16 ± 4.83 mL/min/kg) [26], thus classifying carisoprodol as a low-clearance drug.

Testosterone was used as an experimental control and was fully metabolized within 30 min. In comparison to testosterone (with an experimental $Cl_{\ int\ in\ vitro} = 53$ µL/min/mg), carisoprodol exhibited a significantly slower metabolism.

3.3. Identification of carisoprodol metabolites

In order to identify metabolites of carisoprodol, the chromatograms of the microsomal incubates at different time points were processed using Compound Discoverer software with the MetID workflow. Among the identified metabolites, meprobamate was detected at a R_T of 9.02 min. Its identity was confirmed by comparison with the authentic meprobamate molecule, which provided the same R_T and identical fragmentation spectrum. Additionally, at a R_T of 9.32 min, the principal hydroxylated metabolite of carisoprodol was detected, characterized by a protonated molecular ion at m/z 277.1759 and a sodium adduct at m/z 299.1578 in the MS^1 spectrum. The depletion of carisoprodol and simultaneous increase of meprobamate and hydroxy carisoprodol levels after microsomal incubation of carisoprodol is illustrated in the chromatograms in Fig. 4A and in the graph in Fig. 4B.

Along with the precursor ions of meprobamate and hydroxy carisoprodol, at the same R_T, in-source fragmentation ions were observed in the MS^1 spectra. Specifically, ions at m/z 176.1283 and 158.1177 in both metabolites corresponded to the same *b* and *c* fragments generated for carisoprodol, while an ion at m/z 216.1596 only in the hydroxy carisoprodol spectrum was attributed to the cleavage of the carbonyl C3–O bond within the carbamate moiety (Figure S3, Supplementary Material). Based on these in-source fragments, it could be hypothesized that the hydroxyl group is positioned either on the isopropyl group or on the nitrogen atom of the carbamate, rather than on the *n*-pentyl chain as suggested in the literature. Additionally, five peaks of lower area corresponding to hydroxylated carisoprodol (m/z 277.1754) were detected following hepatic microsomal metabolism, eluting at R_T of 7.96, 8.13, 8.24, 8.43, and 8.61 min.

To confirm that the hydroxyl group is not located on the pentyl side chain of the main hydroxylated metabolite of carisoprodol, as previously suggested in the literature [17,18], deuterated carisoprodol (carisoprodol-d_7) was incubated under the same conditions as the unlabelled compound and the resulting metabolites were analyzed using identical chromatographic and mass spectrometric conditions.

Both deuterated meprobamate (meprobamate-d_7) and deuterated hydroxy carisoprodol (hydroxy carisoprodol-d_7) eluted at the same R_T as their unlabelled counterparts. The $[M+H]^+$ ions for carisoprodol-d_7, meprobamate-d_7, and hydroxy carisoprodol-d_7 were observed at m/z 268.2248, 226.1778, and 284.2197, respectively. The 7.0439 amu mass shift indicated the incorporation of seven deuterium atoms on the pentyl side chain. The MS^2 spectra of both metabolites (Fig. 5B and D), as well as those of their deuterated derivatives (Fig. 5C and E), presented a fragmentation pattern similar to that of the parent compound (Fig. 5A). In particular, the MS^2 spectrum of hydroxy carisoprodol-d_7 presented fragments *c* and *d*, which excluded the presence of the hydroxyl group on the pentyl side chain. Therefore, according to both MS^1 and MS^2 analysis, this finding suggested that hydroxylation likely occurs either on the isopropyl group or on the nitrogen atom of the isopropylcarbamate moiety.

3.4. Comparison of in vitro metabolites with in silico prediction

The metabolites of carisoprodol predicted using GLORYx, a web-based machine learning model for simulating metabolic reaction are shown in the Table 1 in order of the probability score provided by the software.

The results indicate that the metabolite with the highest priority score is hydroxy carisoprodol, with the hydroxyl group at the C4 position of the n-pentyl chain. Other metabolites proposed by the GLORYx software have the same priority as meprobamate, including hydroxy carisoprodol with the hydroxyl group attached to the nitrogen of the carbamate, replaced by isopropyl, or on the tertiary carbon of isopropyl. Additional metabolites were suggested, but with lower priority.

The experimentally identified metabolites only partially matched those predicted *in silico* by GLORYx. In particular, meprobamate was detected both experimentally and among the metabolites predicted by the software.

However, regarding hydroxy carisoprodol, the structure with the highest priority score proposed by GLORYx does not correspond to the

A

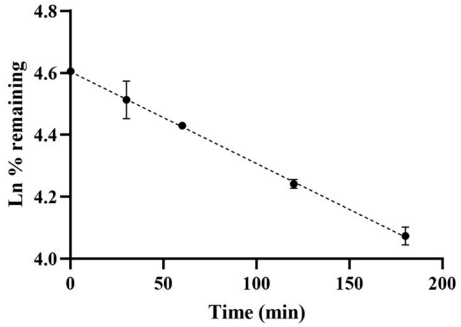

B

Time (min)	Average area of carisoprodol	Normalized peak area (Carisoprodol/IS)	Z (%)	Ln Z	RSD (%)	Linear Regression Equation and Analytical Parameters
0	4.85E+08	5.37E+02	100	4.61	0	
30	4.39E+08	4.98E+02	91.30	4.51	1.34	
60	3.61E+08	4.90E+02	83.89	4.43	0.21	y = -0.0030x + 4.604 R^2 = 0.9804 Slope (k) = 0.0030
120	2.99E+08	4.16E+02	69.53	4.24	0.34	
180	2.91E+08	3.59E+02	58.78	4.07	0.70	

Fig. 3. Metabolic stability of carisoprodol. Linear regression plot obtained by applying the natural logarithm (ln) to the percentage of carisoprodol remaining over incubation time (A); parameters of carisoprodol metabolic stability (B).

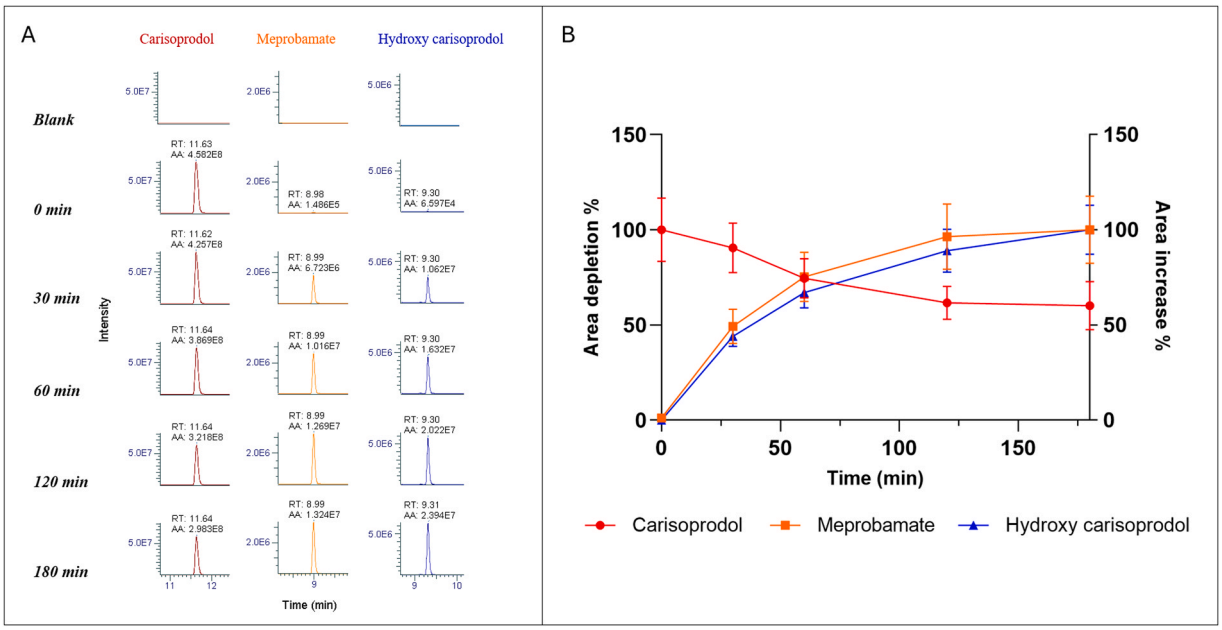

Fig. 4. Depletion of carisoprodol and generation of metabolites in rat liver microsomes. Area of carisoprodol and metabolites (meprobamate and hydroxy carisoprodol) after microsomal incubation of carisoprodol at 0, 30, 60, 120, and 180 min (A); peak area depletion (%) of carisoprodol and peak area increase (%) of meprobamate and hydroxy carisoprodol; 100 % of carisoprodol was set at t = 0, while 100 % of both metabolites was set at t = 180 min (B).

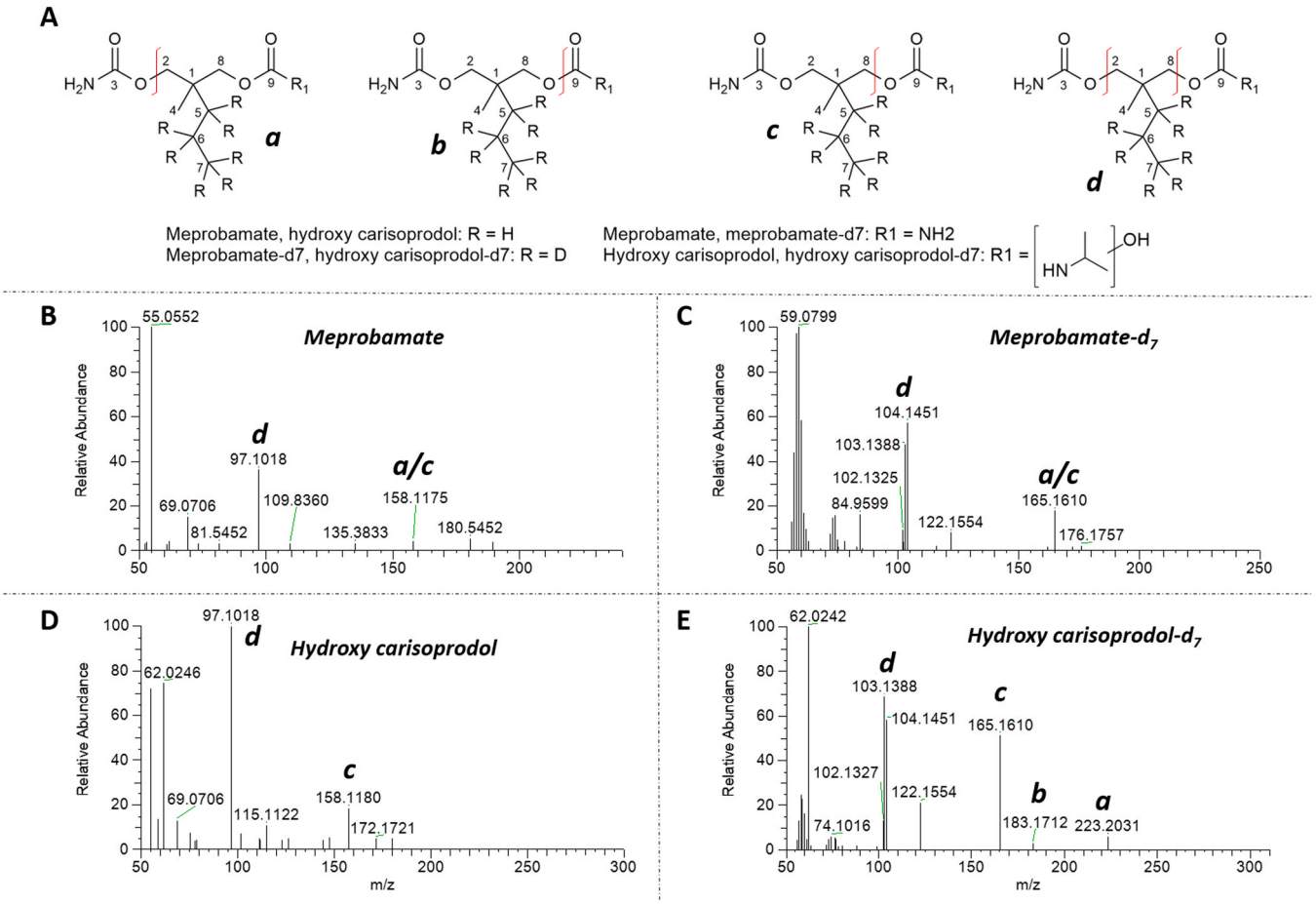

Fig. 5. In-source and MS^2 fragmentation pattern of meprobamate, hydroxy carisoprodol and their deuterated derivatives. Proposed fragmentation pattern for carisoprodol metabolites (A); in-source (MS^2) fragmentation spectrum of meprobamate (B), meprobamate-d_7 (C), hydroxy carisoprodol (D), and hydroxy carisoprodol-d_7 (E).

Table 1
In silico predicted metabolites of carisoprodol (GLORYx) in order of priority score and divided by reaction type.

Priority score		2.184	1.715	1.264	1.19	1.07
Reaction type	Aliphatic hydroxylation	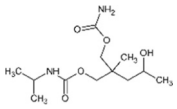	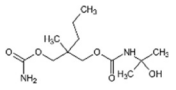	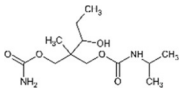	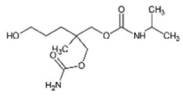	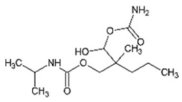
	N-dealkylation		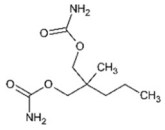			
	Amine hydroxylation		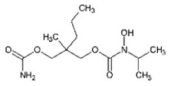			
	Oxidative ether cleavage					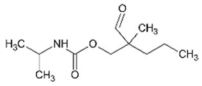

one suggested by the experimental data. Specifically, the principal hydroxylated metabolite could match one of the hydroxylated metabolites predicted in silico by GLORYx, but with a priority score of 1.7. In this prediction, the hydroxyl group would be positioned on the tertiary carbon of the isopropyl group or on the nitrogen atom of the carbamate, rather than on the *n*-pentyl chain, as indicated for the structure with a priority score of 2.2.

4. Conclusions

Carisoprodol is a widely prescribed muscle relaxant, particularly in the United States. More recently, its increasing misuse as a drug of abuse has been reported, prompting the WHO to propose its inclusion in Schedule IV of the 1971 Single Convention on Psychotropic Substances.

Despite being developed in the 1950s, its pharmacokinetics remain poorly understood, as most studies in the literature have focused on its primary metabolite, meprobamate, rather than its hydroxylated metabolite, hydroxy carisoprodol. In this study, we conducted an *in vitro* investigation of the pharmacokinetics of carisoprodol and its major microsomal metabolites. Metabolite profiling revealed that, in addition to meprobamate, several hydroxy derivatives are formed as a result of phase I metabolism. Fragmentation data, supported by deuterated experiments, suggested that hydroxylation occurs on the isopropyl moiety or the carbamate nitrogen, not on the *n*-pentyl chain as previously proposed in literature. The comparison with GLORYx predictions highlighted the limitations of current *in silico* models. While meprobamate was correctly predicted, the incorrect prioritization of hydroxylation sites in hydroxy carisoprodol indicates a need for improved algorithms or hybrid approaches combining machine learning with mechanistic rules. These findings reinforce the necessity of integrated experimental and computational methodologies for accurate metabolic pathway elucidation.

CRediT authorship contribution statement

Maria Angela Vandelli: Resources, Data curation. **Loretta L. Del Mercato:** Funding acquisition. **Cinzia Citti:** Writing – original draft, Supervision, Project administration, Methodology, Investigation, Data curation, Conceptualization. **Giuseppe Cannazza:** Writing – original draft, Supervision, Resources, Project administration, Methodology, Investigation, Funding acquisition, Data curation, Conceptualization. **Elena Ferri:** Writing – original draft, Validation, Investigation, Formal analysis. **Cristian Caprari:** Validation, Investigation, Formal analysis.

Declaration of Competing Interest

The authors declare that they have no known competing financial interests or personal relationships that could have appeared to influence the work reported in this paper.

Acknowledgements

This work received funding from the Italian Ministry of Research (MUR) in the framework of the National Recovery and Resilience Plan (NRRP) under the complementary actions to the NRRP "Fit4MedRob" Grant (PNC0000007, n. B53C22006960001) funded by NextGenerationEU.

Moreover, the work was supported by Fondo Di Ateneo Per La Ricerca Anno 2024 (FAR2024PD) funded by the Department of Life Sciences of the University of Modena and Reggio Emilia (A. D06@FAR2024_DIP@05FA-CANNAZZA_FARDIP_2024).

The authors acknowledge Dr. Diego Pinetti for his technical support and the "Fondazione Cassa di Risparmio di Modena" for funding the UHPLC-QExactive system at the Centro Interdipartimentale Grandi Strumenti (CIGS) of the University of Modena and Reggio Emilia.

The authors also acknowledge Marco Grasso for his contribution and support to the data organization.

Appendix A. Supporting information

Supplementary data associated with this article can be found in the online version at doi:10.1016/j.jpba.2025.117091.

Data availability

Data will be made available on request.

References

[1] Z. Amin, S. Zulkifly, S.D. Iskandar, Carisoprodol intoxication: a comprehensive review, Crit. Care Shock 22 (2019) 197–203.
[2] Y. Li, C. Delcher, J.D. Brown, Y.-J. Wei, G.M. Reisfield, A.G. Winterstein, Impact of schedule IV controlled substance classification on carisoprodol utilization in the United States: an interrupted time series analysis, Drug Alcohol Depend. 202 (2019) 172–177, https://doi.org/10.1016/j.drugalcdep.2019.05.025.
[3] Carisoprodol - referral | European Medicines Agency (EMA), (2007). ⟨https://www.ema.europa.eu/en/medicines/human/referrals/carisoprodol⟩ (accessed July 17, 2025).
[4] WHO Expert Committee on Drug Dependence: Forty-seventh report, (2025). ⟨https://www.who.int/publications/i/item/9789240107649⟩ (accessed July 17, 2025).
[5] S.A. Tse, R.S. Atayee, B.M. Best, A.J. Pesce, Evaluating the relationship between carisoprodol concentrations and meprobamate formation and Inter-Subject and

Intra-Subject variability in urinary excretion data of pain patients, J. Anal. Toxicol. 36 (2012) 221–231, https://doi.org/10.1093/jat/bks018.
[6] Drugs@FDA: FDA-Approved Drugs, (n.d.). ⟨https://www.accessdata.fda.gov/scripts/cder/daf/index.cfm?event=overview.process&ApplNo=011792⟩ (Accessed February 26, 2025).
[7] S. Simon, C. D'Andrea, W.J. Wheeler, H. Sacks, Bioavailability of oral carisoprodol 250 and 350 mg and metabolism to meprobamate: a single-dose crossover study, Curr. Ther. Res. 71 (2010) 50–59, https://doi.org/10.1016/j.curtheres.2010.02.003.
[8] A. Calvo, S. Alonso, E. Prieto, A. Ascaso-Del-Rio, J. Ortuño, N. Fernandez, A. Portolés, Single and multiple dose PK-PD characterization for carisoprodol. Part I: pharmacokinetics, metabolites, and 2C19 phenotype influence. Double-blind, Placebo-Controlled clinical trial in healthy volunteers, J. Clin. Med. 11 (2022) 858, https://doi.org/10.3390/jcm11030858.
[9] T. Lewandowski, Pharmacokinetic modeling of carisoprodol and meprobamate disposition in adults, Hum. Exp. Toxicol. 36 (2017) 846–853, https://doi.org/10.1177/0960327116672912.
[10] J.K. Hicks, K. Sangkuhl, J.J. Swen, V.L. Ellingrod, D.J. Müller, K. Shimoda, J. R. Bishop, E.D. Kharasch, T.C. Skaar, A. Gaedigk, H.M. Dunnenberger, T.E. Klein, K.E. Caudle, J.C. Stingl, Clinical pharmacogenetics implementation consortium guideline (CPIC) for CYP2D6 and CYP2C19 genotypes and dosing of tricyclic antidepressants: 2016 update, Clin. Pharmacol. Ther. 102 (2017) 37–44, https://doi.org/10.1002/cpt.597.
[11] L. Dean, M. Kane, Carisoprodol Therapy and CYP2C19 Genotype, in: V.M. Pratt, S. A. Scott, M. Pirmohamed, B. Esquivel, B.L. Kattman, A.J. Malheiro (Eds.), Med. Genet. Summ., National Center for Biotechnology Information (US), Bethesda (MD), 2012. ⟨http://www.ncbi.nlm.nih.gov/books/NBK425390/⟩ (accessed February 27, 2025).
[12] J.G. Bramness, S. Skurtveit, M. Gulliksen, H. Breilid, V.M. Steen, J. Mørland, The CYP2C19 genotype and the use of oral contraceptives influence the pharmacokinetics of carisoprodol in healthy human subjects, Eur. J. Clin. Pharmacol. 61 (2005) 499–506, https://doi.org/10.1007/s00228-005-0970-1.
[13] H. Olsen, E. Koppang, G. Alvan, J. Morland, Carisoprodol elimination in humans, Ther. Drug Monit. 16 (1994) 337. ⟨https://journals.lww.com/drug-monitoring/abstract/1994/08000/carisoprodol_elimination_in_humans.1.aspx⟩ (accessed February 27, 2025).
[14] L.A. Gonzalez, M.B. Gatch, C.M. Taylor, C.L. Bell-Horner, M.J. Forster, G.H. Dillon, Carisoprodol-Mediated modulation of GABAA receptors: in vitro and in vivo studies, J. Pharmacol. Exp. Ther. 329 (2009) 827–837, https://doi.org/10.1124/jpet.109.151142.
[15] J.F. Douglas, B.J. Ludwig, A. Schlosser, The metabolic fate of carisoprodol in the dog, J. Pharmacol. Exp. Ther. 138 (1962) 21–27, https://doi.org/10.1016/S0022-3565(25)26382-0.
[16] T. Matsumoto, T. Sano, T. Matsuoka, M. Aoki, Y. Maeno, M. Nagao, Simultaneous determination of carisoprodol and acetaminophen in an attempted suicide by liquid Chromatography-Mass spectrometry with positive electrospray ionization, J. Anal. Toxicol. 27 (2003) 118–122, https://doi.org/10.1093/jat/27.2.118.
[17] J. Edelson, A. Schlosser, J.F. Douglas, Structure of the metabolite of carisoprodol, hydroxycarisoprodol, Biochem. Pharm. 14 (1965) 901–902, https://doi.org/10.1016/0006-2952(65)90114-0.
[18] W. Skinner, D. McKemie, S. Stanley, Quantitative determination of carisoprodol and its metabolites in equine urine and serum by liquid Chromatography-Tandem mass spectrometry, Chromatographia 59 (2004) S61–S67, https://doi.org/10.1365/s10337-004-0244-6.
[19] C. Stork, G. Embruch, M. Šícho, C. de Bruyn Kops, Y. Chen, D. Svozil, J. Kirchmair, NERDD: a web portal providing access to in silico tools for drug discovery, Bioinformatics 36 (2020) 1291–1292, https://doi.org/10.1093/bioinformatics/btz695.
[20] Advanced Chemistry Development, Inc., ACD/ChemSketch (Freeware Version 2024.2.0) Toronto (ON), (2024). ⟨https://www.acdlabs.com⟩.
[21] C. de Bruyn Kops, M. Šícho, A. Mazzolari, J. Kirchmair, GLORYx: prediction of the metabolites resulting from phase 1 and phase 2 biotransformations of xenobiotics, Chem. Res. Toxicol. 34 (2021) 286–299, https://doi.org/10.1021/acs.chemrestox.0c00224.
[22] K.M. Knights, D.M. Stresser, J.O. Miners, C.L. Crespi, In vitro drug metabolism using liver microsomes, 7.8.1-7.8.24, Curr. Protoc. Pharm. 74 (2016), https://doi.org/10.1002/cpph.9.
[23] Thermo Fisher Scientific Inc, Compound Discoverer 3.3 SP3 Waltham (MA): Thermo Fisher Scientific, (2024). ⟨https://www.thermofisher.com⟩.
[24] L.W.T. Tang, E.C.Y. Chan, Quantification of the irreversible fibroblast growth factor receptor inhibitor futibatinib by UPLC-MS/MS: application to the metabolic stability assay in human liver microsomes for the estimation of its in vitro hepatic intrinsic clearance, J. Pharm. Biomed. Anal. 214 (2022) 114731, https://doi.org/10.1016/j.jpba.2022.114731.
[25] A.B. Godoi, N. de J. Antunes, K.F. Cunha, A.F. Martins, M.A. Huestis, J.L. Costa, Metabolic stability and metabolite identification of N-Ethyl pentedrone using rat, mouse and human liver microsomes, Pharmaceutics 16 (2024) 257, https://doi.org/10.3390/pharmaceutics16020257.
[26] P. Dalén, G. Alvan, M. Wakelkamp, H. Olsen, Formation of meprobamate from carisoprodol is catalysed by CYP2C19, Pharmacogenetics 6 (1996) 387–394, https://doi.org/10.1097/00008571-199610000-00002.